

Electronic Supplementary Information:

**Enhanced uptake of glyoxal at acidic nanoparticle interface:
implications for secondary organic aerosol formation**

Qiuju Shi,^{a†} Weinan Zhang,^{a†} Yuemeng Ji,*^a Jiaxin Wang,^a Dandan Qin,^a Jiangyao Chen,^{a,b} Yanpeng Gao,^a

Guixing Li^{a,b} and Taicheng An^a

^a Guangdong Key Laboratory of Environmental Catalysis and Health Risk Control, Guangzhou Key Laboratory Environmental Catalysis and Pollution Control, School of Environmental Science and Engineering, Institute of Environmental Health and Pollution Control, Guangdong University of Technology, Guangzhou 510006, China

^b Synergy Innovation Institute of GDUT, Shantou 515041, China.

[†] Both authors contributed equally to this work.

*Corresponding Author: Prof. Yuemeng Ji

Tel: 86-20-39322291

E-mail: jiym@gdut.edu.cn

Methods

The choice of SA concentration

The previous studies showed that the cloud sample in the atmosphere was acidic.¹ The acidity of nanoparticles varies from 60 wt% to 80 wt% in the upper troposphere and decreases in the lower troposphere.^{2,3} Given the condition in the atmosphere, the different concentrations of SA (20 wt%, 30 wt%, 50wt% and 60 wt%) were investigated in the work. According to the density table of SA, the corresponding density of solution of SA from 20 wt% to 60 wt% is 1.136, 1.215, 1.391 and 1.494 g cm⁻³, respectively. The concentrations of SA ([SA]) were calculated as follows:

$$c = \frac{1000 \rho \text{ wt}\%}{M}$$

(1)

where the ρ and M represent the density of solution of SA and molar mass of molecule, respectively.

The angular distribution

The specific property of GL at the interface is the difference of polarization relative to the bulk water because of the discrepancy of orientation of GL at the interface. Thus, a key factor in the orientation of GL at the interface is its angular distribution. The Z-axis was defined as the axis perpendicular to the nanoparticle interface and ϑ as the angle formed between the Z-axis and the C=O bond. The total energy was changed with the simulation time by the trajectory analysis at the interface. The most stable configurations were confirmed by the change of the total energy of every typical snapshot and the 100 typical snapshots from the most stable configurations were chosen to observe the angle distribution of C=O bond.

The radial distribution function and coordination number

The radial distribution function (RDF) can be used to estimate the strength of the hydrogen-bonding (HB) between special atoms. The HB between GL and water at the interface in the neutral and acidic systems occurs. The number of water around the GL molecule was obtained by calculating the coordination number (N). Considering the density at the interface is equal to 50% of the nanoparticle interior,⁴ the N parameter is obtained as the integrations of $g(r)$ within $r=2.5$ Å.

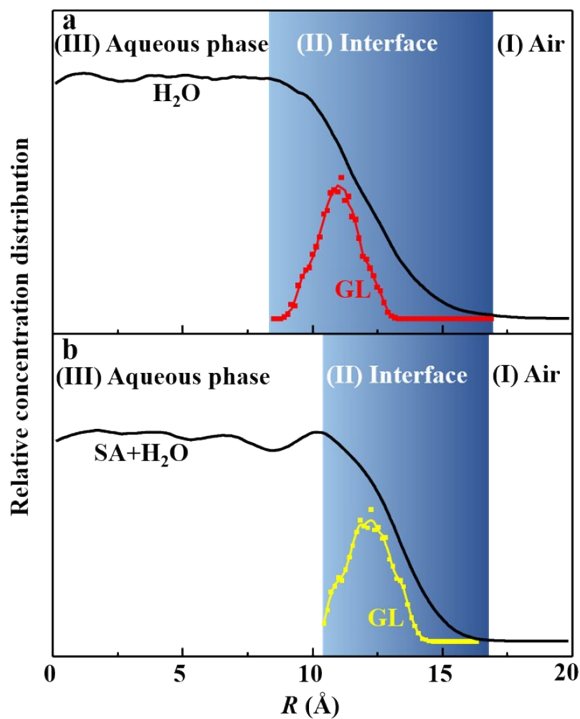


Fig. S1 Relative concentration distribution of GL and the corresponding solvent at (a) the A-N interface and (b) the A-A interfaces.

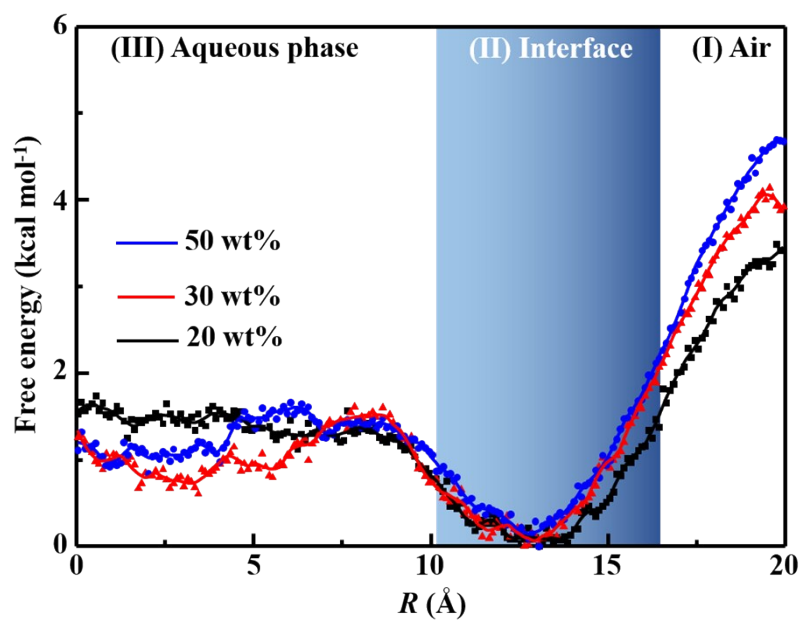


Fig. S2 The free energy profile of gaseous GL approaching into acidic nanoparticles with the different concentrations of SA (20 wt% (black), 30 wt% (red), and 50 wt% (blue)).

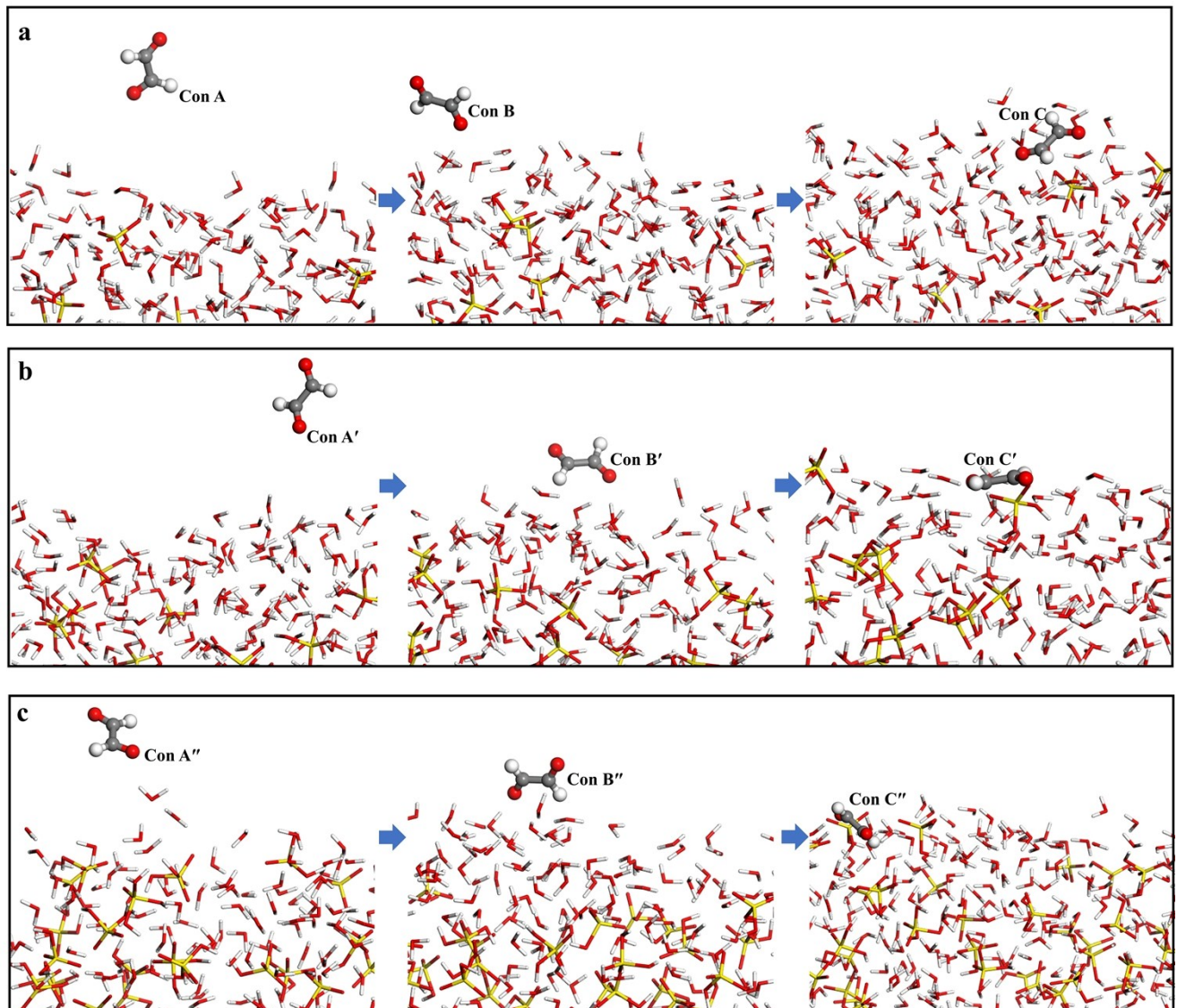


Fig. S3 Typical snapshots along with the trajectories of gaseous GL to the acidic nanoparticles with the concentrations of SA (a) 20 wt%, (b) 30 wt% and (c) 50 wt%, respectively. The Con A, Con A' and Con A'' are snapshots at the point of the maximum free energy in acidic system; the Con B, Con B' and Con B'' correspond to the snapshots at the A-A surface which are the bounds between gas phase and interface, and the Con C, Con C' and Con C'' represent the most stable structures at the acidic nanoparticle interface.

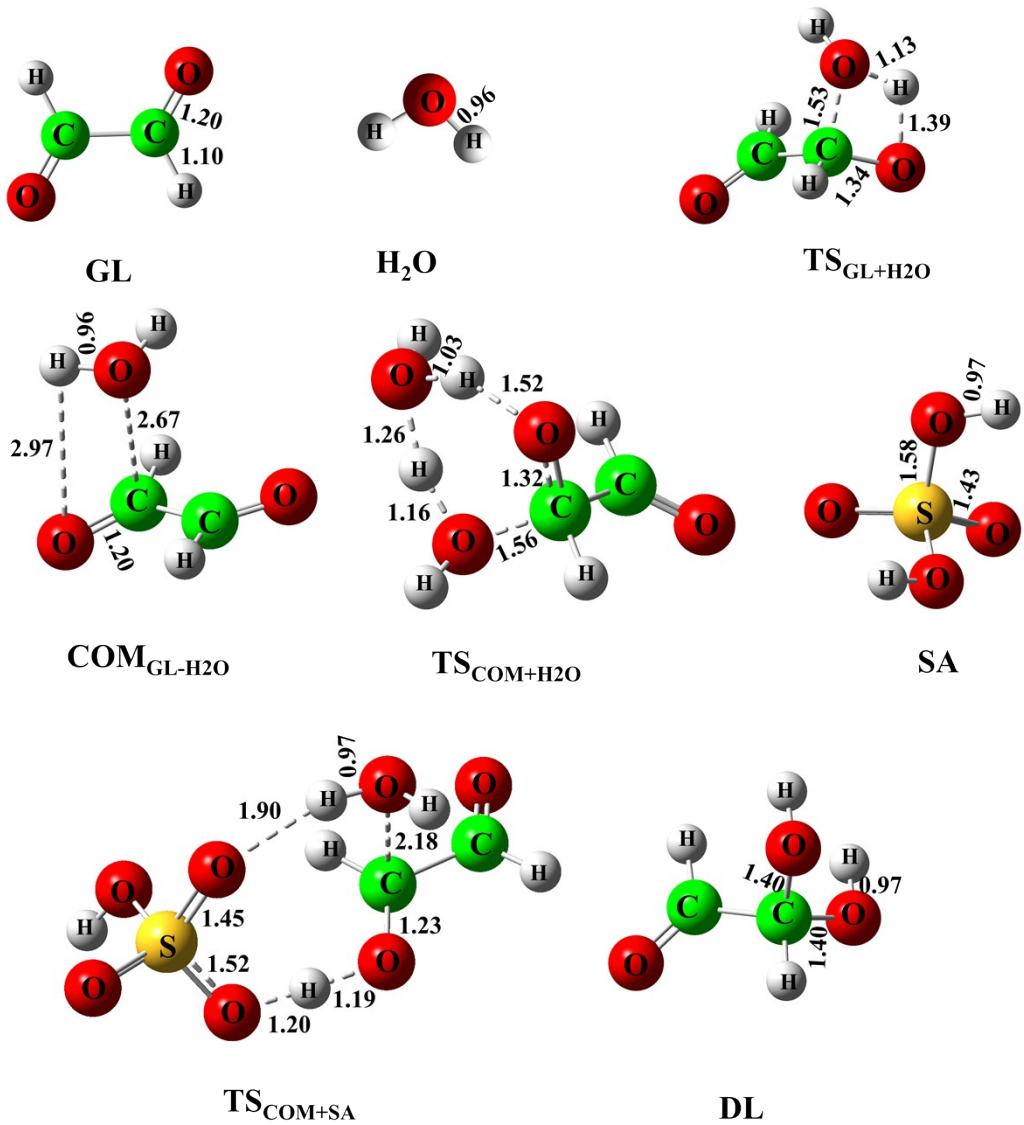


Fig. S4 The optimized geometries of the reactants, complex, transition states and products at the M06-2X/6-311G(d,p) level. The unit of the bond length is Å.

Table S1 Numbers of SA (N_1) and water (N_2) molecules under the acidic nanoparticles with the different concentrations of SA ([SA]) between 20 wt% to 60 wt%. The length of the box is 26 Å.

wt%	N_1	N_2	^a [SA]	^b Density
20	25	535	2.319	1.136
30	39	501	3.719	1.215
50	75	409	7.097	1.391
60	97	352	9.147	1.494

^aThe unit is mol L⁻¹.

^bThe value is the density of the corresponding solution of SA and the unit is g cm⁻³.

Table S2 Coordination numbers (N) of water molecules in the first solvation shell for $O_{\text{GL}}-\text{H}_{\text{water}}$ at the interface and in the nanoparticle interior region in the neutral and acidic systems.

System	Phase	N
neutral	interface	2.9
acidic	interface	2.2
neutral	nanoparticle interior	6.0
acidic	nanoparticle interior	6.3

Table S3 Cartesian coordinates, vibrational frequencies (in cm^{-1}), absolute energies (in hartrees), and thermal corrections (in hartrees) of stationary points in the reactions of GL and H_2O and SA at the M06-2X/6-311G(d,p) level.

Species	Cartesian coordination				Absolute energies	Thermal corrections	Frequencies
GL	C	0.95816500	-0.57721300	-0.00012400	-227.7966871	0.011649	136, 333, 571, 842, 1097, 1103, 1354, 1402, 1822, 1854, 3067, 3073
	H	1.17429600	-1.65771000	-0.00003700			
	C	-0.51528800	-0.20165000	0.00008800			
	O	1.80656400	0.27429600	0.00008200			
	O	-1.36402900	-1.05294600	0.00003600			
	H	-0.73085400	0.87886100	0.00021000			
H_2O	O	2.26394800	0.30023000	0.00000000	-76.4257234	0.003105	1602, 3859, 3936
	H	3.22450700	0.35184600	0.00000000			
	H	1.99188700	1.22300900	0.00000000			
$\text{TS}_{\text{GL+H}_2\text{O}}$	C	0.98946300	-0.09102100	-0.36642000	-304.1777444	0.032456	-1412, 79, 300, 339, 424, 472, 725, 839, 961, 1037, 1160, 1191, 1277, 1318, 1356, 1428, 1837, 2193, 3046, 3117, 3718
	H	0.86275300	-0.22369100	-1.45619300			
	C	-0.29924500	0.16337300	0.39256400			
	O	2.06809800	-0.06047100	0.16619600			
	O	-1.02066500	1.16173800	-0.14913800			
	O	-1.30790700	-0.94836800	0.08144000			
	H	-1.75153500	-0.00559500	-0.36044300			
	H	-1.01671800	-1.57654100	-0.60415600			
	H	-0.15202300	0.14852100	1.47595000			
$\text{COM}_{\text{GL-H}_2\text{O}}$	C	0.33204600	-0.80846700	0.39379100	-304.2316561	0.031483	112, 144, 154, 177, 179, 337, 364, 396, 565, 866, 1096, 1106, 1344, 1392, 1601, 1811, 1851, 3062, 3068, 3841, 3919
	H	0.27547700	-0.66571900	1.48538200			
	C	-0.84842700	-0.26634400	-0.39442200			
	O	1.23375300	-1.38453300	-0.15677000			
	O	-1.85897900	0.07103300	0.16471800			
	O	0.78939000	1.79101800	-0.10529600			

	H 0.51209700 2.00229200 0.79350000 H 1.71542200 1.54182200 -0.00837200 H -0.71803100 -0.24967500 -1.48794100			
TS _{COM+H2O}	C 0.32777800 0.31873300 -0.61484500 H 0.87766000 1.03123300 -1.24130800 C 1.24142200 -0.32114600 0.41723200 O -0.40719900 -0.58552700 -1.22840600 O 2.44345300 -0.22780800 0.38696000 H 0.72077100 -0.95515500 1.15988200 O -2.13638400 -0.50810900 0.53615400 H -1.95913700 -1.07063900 1.30149100 H -1.53465200 -0.83956200 -0.23887800 O -0.54910300 1.24215900 0.29048500 H -0.90674000 1.96021000 -0.25343200 H -1.41924200 0.52267000 0.57637600	-380.6462366	0.054379	-868, 42, 79, 297, 339, 364, 405, 444, 506, 531, 648, 754, 789, 985, 1003, 1053, 1168, 1250, 1337, 1357, 1421, 1532, 1610, 1735, 1831, 2562, 3023, 3048, 3788, 3849
SA	O 0.34271300 -0.83513700 1.21135500 S -0.00005600 -0.14498600 0.00156800 O -0.34333500 -0.86212700 -1.19224100 O 1.16968600 0.82708300 -0.42095700 O -1.16908900 0.83709700 0.40229300 H 1.55806000 1.29539100 0.34063500 H -1.55696500 1.28905000 -0.36932500	-700.211748	0.010715	266, 335, 388, 443, 491, 527, 551, 864, 903, 1122, 1142, 1213, 1400, 3711, 3722
TS _{COM+SA}	C -1.74116900 -0.46015500 -0.04347400 O -1.66331000 1.71046000 -0.21596500 O -1.16465400 -0.91681300 -1.03587600 H -1.24542000 -0.35510600 0.92541000 H 0.01240400 -1.03691800 -0.86901900 O 1.13161300 1.26833500 -0.15679700	-1004.4584404	0.062562	-583, 46, 61, 93, 106, 122, 160, 211, 219, 280, 300, 311, 346, 420, 430, 473, 551, 567, 586, 612, 718, 748, 865, 953, 1051, 1088, 1130, 1151, 1247, 1272, 1329, 1365, 1400, 1552, 1611,

	H -0.69632800 1.77776400 -0.13879400 O 1.19072500 -1.12710100 -0.67500300 S 1.88027500 0.03557200 0.01433200 O 1.73077500 -0.27207500 1.57339300 O 3.28525500 0.04577500 -0.32072300 H -1.84451100 1.89734800 -1.14724800 H 2.20806600 -1.08032900 1.82871300 C -3.24754700 -0.32508600 -0.07361500 H -3.69640400 -0.27202000 -1.07659300 O -3.87164300 -0.30713600 0.94981400			1707, 1859, 3099, 3168, 3712, 3754, 3853
DL	C 0.93879800 0.00188800 0.37583400 H 0.85603100 0.00452800 1.48016800 C -0.39162100 0.00004700 -0.35765900 O 2.00534800 0.00001900 -0.18286600 O -1.09603300 -1.17025800 -0.03367400 O -1.09925800 1.16841200 -0.03467400 H -1.19500400 -1.21360800 0.92729000 H -1.19698400 1.21224600 0.92651500 H -0.22756200 -0.00015300 -1.43330500	-304.2499671	0.039282	88, 328, 381, 386, 411, 462, 635, 1026, 1049, 1218, 1226, 1303, 1328, 1438, 1454, 1457, 1846, 3004, 3169, 3811, 3813

References

1. J. Guo, Y. Wang, X. Shen, Z. Wang, T. Lee, X. Wang, P. Li, M. Sun, J. L. Collett, W. Wang and T. Wang, Characterization of cloud water chemistry at Mount Tai, China: Seasonal variation, anthropogenic impact, and cloud processing, *Atmos. Environ.*, 2012, **60**, 467-476.
2. J. Curtius, B. Sierau, F. Arnold, M. de Reus, J. Ström, H. A. Scheeren and J. Lelieveld, Measurement of aerosol sulfuric acid: 2. Pronounced layering in the free troposphere during the second Aerosol Characterization Experiment (ACE 2), *J. Geophys. Res. Atmos.*, 2001, **106**, 31975-31990.
3. R. L. Tanner, B. P. Leaderer and J. D. Spengler, Acidity of atmospheric aerosols, *Environ Sci Technol.*, 1981, **15**, 1150-1153.
4. J. Zhong, M. Kumar, J. M. Anglada, M. T. C. Martins-Costa, M. F. Ruiz-Lopez, X. C. Zeng and J. S. Francisco, Atmospheric Spectroscopy and Photochemistry at Environmental Water Interfaces, *Annu Rev Phys Chem*, 2019, **70**, 45-69.